Current Trends in Biotechnology and Pharmacy
Vol. 19(4) 2603-2620, October 2025, ISSN 0973-8916 (Print), 2230-7303 (Online)
DOI: 10.5530/ctbp.2025.4.41



# Enhanced Skin Permeation of Bisoprolol Fumarate Using a Microneedle-Assisted Transdermal Patch with Chemical Penetration Enhancers for Potential Hypertensive Effect

**Amina Aziz[1], Maryam Shabbir[1], Uzair Nagra[2], Ayesha Mahmood[1], Atika Afzal[1], Ali Abbasi Moghadam[1], Shazia Ashraf[3], Muhammad Arslan Amjad[4], Muhammad Ali Khan Sherwani[1], Muhammad Asis Ullah Khan[1]**

[1]Faculty of Pharmacy, The University of Lahore, Lahore, Pakistan
[2]Medisearch Pharmacal Pvt. Ltd., Lahore, Pakistan
[3]Department of Pharmaceutics, The Islamia University of Bahawalpur, Bahawalpur, Pakistan
[4]Department of Pharmaceutical Sciences, Superior University, Lahore, Pakistan

* Corresponding author: maryam.shabbir@pharm.uol.edu.pk

## Abstract

Bisoprolol fumarate (BF) can be administered transdermally to control hypertension in elderly and postoperative settings, but the delivery is blunted due to the hydrophilic nature of the drug across the hydrophobic skin barrier. The present study was aimed at evaluating and optimizing the matrix-type transdermal patch of BF using Eudragit L100 and HPMC as polymers and PEG 400 as a plasticizer. The patches were evaluated for organoleptic characteristics, moisture analysis, and in vitro permeation studies across synthetic membranes. Based on desired characteristics, the HPMC: Eudragit L100 (5:1) patch was further loaded with permeation enhancers, such as Span 20, orange oil, and oleic acid, by the solvent casting method. The patches showed desired physicochemical properties and moisture content. However, BO1 released 6864.17 µg/cm² (equivalent to 8237.0 µg) of drug in 24 hours, which was better than other formulations. The ex vivo permeation analysis demonstrated that Span 20 at 12% w/w (BO1-S12) favored the highest permeation of BF across excised rabbit skin (5974.0 µg/cm²) as compared to the control patch (3517.0 µg/cm²). However, to improve the BF permeation, a parallel micropore (solid microneedles) and intact skin transport pathway was adapted. The pretreatment of skin with solid microneedles improved the BF cumulative permeation (7580.0 µg/cm²) and flux (225.67 µg/cm²/hr) as compared to BO1-S12 (195.11 µg/cm²/hr). The finding suggests that it is advantageous to use microneedles to create microchannels in the skin that would let drugs penetrate deeper into the dermis for systemic absorption. Therefore, the combination of microneedles with a permeation enhancer effectively sustains BF delivery over 24 hours with minimal skin irritation and desirable storage stability.

**Keywords:** Bisoprolol fumurate, Span 20, Solid microneedle, skin permeation, transdermal patch

## Introduction

Hypertension (HTN) is defined as a "persistent elevation in blood pressure above a certain threshold value of 140/90 mm Hg" (1). HTN is a major global cause of mortality and morbidity, causing nearly 9 million deaths annually. According to the World Health Organization (WHO) report, only 54% of adults are diagnosed, whereas only 42% of patients receive treatment for hypertension, and a mere 21% have their hypertension controlled through medication or

diet control (2). In Pakistan, two epidemiological studies, the 1990–1994 National Health Survey and the hypertension studies in rural northern areas (2008-2015), reported disease prevalence rates of 19.1% and 14%, respectively (3). HTN has been linked to various disorders, including cardiovascular disease, atrial fibrillation, heart failure, angina pectoris, chronic kidney disease, and diabetes mellitus. Antihypertensive therapy, including angiotensin receptor blockers, calcium channel blockers, angiotensin-converting enzyme (ACE) inhibitors, and thiazide-type diuretics, can reduce the risk of these disorders (4). Traditional dosage forms, such as tablets and capsules, can be challenging for hypertensive patients, especially in pediatric populations with difficulty swallowing or needle phobias. The use of transdermal microneedle-based drug delivery systems can help address these issues. The purpose of transdermal dosage design is to increase the permeation of drug across the skin with a consistent serum-drug level via the stratum corneum. The drug may remain in the viable epidermis and dermis for local effect or may pass into the systemic circulation, concurrently minimizing the degradation and metabolism of the drug (5).

Bisoprolol fumarate (BF) is a $\beta_1$ blocker, with a molecular weight of 383.48 kDa. It is considered to be of high therapeutic value and is most frequently used in the management of heart failure and high blood pressure. Japanese guidelines indicate that the sudden cessation of oral β-blocker therapy can exacerbate heart disease and that abrupt discontinuation of oral therapy of β-blockers leads to worsening of the heart disease (6). Furthermore, the significant hydrophilicity of BF impedes its penetration through the stratum corneum, the lipophilic outer layer of the skin. Therefore, it is essential to develop a formulation that effectively bypasses the stratum corneum and delivers the drug directly to the hydrophilic layers of the skin, specifically the viable epidermis and dermis, for subsequent absorption into the systemic circulation.

The transdermal administration of BF may provide more constant and prolonged plasma levels as compared to the oral dosage form (7). In one of the settings, ion-pair strategy has been reported to increase BF permeation through transdermal patch (8). Alternatively, chemical permeation enhancers have been extensively studied to increase the transdermal flux of hydrophilic drugs such as BF, including propylene glycol (PG), dimethyl sulphoxide (DMSO), and Tween 80 (9). However, they are sometime ineffective in delivering hydrophilic drugs across stratum corneum since their potencies are drug-specific. Therefore, the pretreatment of skin with solid microneedles can form local skin depot in the micropores for continuous drug delivery. The ability of the chemical permeation enhancers to disrupt the skin barrier would allow the conitnuious delivery of BF even after the micropores close with the passage of time. Due to possible higher demand of BF patch, the present study reports a matrix transdermal patch of BF by using hydrophilic (HPMC) and hydrophobic polymers (Eudragit L100) with different permeation enhancers such as nonionic surfactant (Span 20), unsaturated fatty acid (Oleic acid), and terpenes (orange oil) to facilitate the passage of drug through the microneedle pretreated skin in terms of cumulative drug release and flux. Also, to the best of our knowledge, no characterization of BF transdermal patch has been done using pre-treatment of microneedle.

## Material and method

Bisoprolol fumarate (BF) (generous gift from Mass Pharma Pvt. Ltd., Lahore, Pakistan). Polyvinyl alcohol (PVA), polyethylene glycol 400 (PEG 400), Eudragit L-100, hydroxypropyl methylcellulose (HPMC), sodium chloride were bought from Merck Germany. Sodium hydroxide, potassium dihydrogen phosphate, disodium hydrogen phosphate, potassium chloride, and calcium chloride were bought from Sigma-Aldrich, USA. Silica beads were boght from Uni chem., India and hydrochloric acid and methanol from BDH England.

***Ethical approval and husbandary***

The protocols pertaining to animal usage were approved by the Institutional Research Ethical Committee (IREC), The University of Lahore, Lahore, Pakistan, under the protocol number IREC-2017-22. The pathogen-free male albino rabbits, weighing approximately 2.25 kg each with an age of 24-25 weeks, were procured from the Animal House, Faculty of Pharmacy, The University of Lahore, Lahore, Pakistan. The animal handling and study were performed according to the guidelines outlined in "The Principles of Laboratory Animal Care," NIH. Upon procurement, the rabbits were given two weeks to acclimatize to the surroundings (25±1°C, 12:12 light-dark cycle, >30% RH). The animals were provided with adequate food and water and housed in stainless steel cages that were littered down with straw. Before the start of experimentation, the rabbits were clinically examined for any sign of disease or emaciation.

***Fabrication of matrix transdermal patch of BF***

The patches were prepared by solvent evaporation technique as described previously. To find the appropriate concentration of Eudragit L-100 and HPMC, several polymer ratios were used, as shown in Table 1. The polymers were dissolved in 10 ml of methanol using a hot plate magnetic stirrer at 32±2°C until a transparent solution was obtained. Later, PEG 400 was added as a plasticizer and blended for 15 minutes. To get a homogeneous solution, the medication was first dissolved in 5 ml of methanol and then slowly added to the polymeric solution. After thoroughly mixing, the drug-polymer solution was placed onto a previously prepared petri dish containing dried PVA backing layer (4% w/v). The petri dish was covered with a funnel to control the rate of methanol evaporation and dried in a desiccator at room temperature for 12 hours. After the drying process, the patches were carefully removed from the petri dishes and stored in a closed container till further analysis.

Table 1: Formulation of optimized transdermal patch of Bisoprolol

| Formulation | E L-100: HPMC (mg) | Drug (mg) | PEG 400 (mg) | Penetration enhancer (w/w) | Methanol (ml) |
|---|---|---|---|---|---|
| BO1 | 1:5 | 10 | 240 | - | 15 |
| BO2 | 2:4 | 10 | 240 | - | 15 |
| BO3 | 3:3 | 10 | 240 | - | 15 |
| BO4 | 4:2 | 10 | 240 | - | 15 |
| BO5 | 5:1 | 10 | 240 | - | 15 |
| BO1-S9 | 1:5 | 10 | 240 | Span 20 (9%) | 15 |
| BO1-S12 | 1:5 | 10 | 240 | Span 20 (12%) | 15 |
| BO1-O9 | 1:5 | 10 | 240 | Orange oil (9%) | 15 |
| BO1-O12 | 1:5 | 10 | 240 | Orange oil (12%) | 15 |
| BO1-A9 | 1:5 | 10 | 240 | Oleic acid (9%) | 15 |
| BO1-A12 | 1:5 | 10 | 240 | Oleic acid (12%) | 15 |
| BO1-S12-M | 1:5 | 10 | 240 | Span 20 (12%) | 15 |

Based on organoleptic and other physicochemical properties, Eudragit L-100: HPMC (1:5) was chosen for the further processing of the BF transdermal patches. To better understand the effect of permeation enhancers, a mixture of the two polymers was formulated with Span 20, orange oil, and oleic acid at concentrations of 9% or 12% w/w as shown in Table 1.

***Organoleptic and physicochemical characteristics of BF transdermal patch***

The patches were visually inspected to determine their gloss, transparency, translucency, smoothness, flexibility, and homogeneity. A grading system was developed, with (+++) signifying the most desirable and targeted attribute and (+) denoting the least desired outcomes.

A digital vernier caliper was used to measure the patch's thickness to confirm its wearability and flexibility (n=10). The BF patch was measured at three different points, and the average and standard deviation were calculated. Additionally, the BF patches (n=20) were weighed on an electronic weighing balance to ensure weight homogeneity.

To test surface pH, each monolithic film was swollen with 0.5 mL of distilled water for 1 hour at room temperature. The electrode was then brought into contact with the film's surface and allowed to equilibrate for 1 minute in order to measure the surface pH.

***Moisture analysis of BF transdermal patch***

The determine the amount of moisture retained after drying, the transdermal patches were evaluated for moisture content and moisture uptake studies. To measure moisture content, the films (n=5) of 1×1 cm were individually weighed () and stored in an incubator containing silica beads at 25±2°C. The BF patches were weighed () again after a predetermined time, and their moisture content (%) was estimated according to the equation:

Similarly, to estimate the moisture uptake during storage, the films (n=5) of 1×1 cm were weighed () and stored in an incubator with a saturated solution of potassium chloride (KCl) at 84% relative humidity (RH) for five days. The BF films were weighed again () after a predetermined time and the percentage moisture uptake was estimated according to the equation: (10)

$$Moisture\ uptake\ (\%) = W_i - W_f / W_f \times 100$$

***Water vapor estimation of BF transdermal patch***

To estimate the water vapor transmission rate (WVTR), the films (n=5) of 1×1 cm were individually weighed () on a sensitive weighing balance. The film was fixed to the brim of a tared vial containing 5 g of fused calcium chloride ($CaCl_2$). The loaded-vials were weighed and stored in an incubator loaded with 200 mL of KCl solution at 32±2ºC and 84% RH. The vials were weighed () after 24 hours to calculate WVTR using the following equation:

$$WVTR\ (\%) = W_f - W_i / (A \times t) \times 100$$

Where; A = surface area in cm2; and t = time (h) (11).

To estimate water vapor permeability (WVP), each 1x1 cm film (*n*=5) was weighted individually () on a sensitive weighing balance. Silica beads were placed in a 5 ml tared vial, and polymeric films were attached to the brim of the vial with double-tape. The vials were weighed and stored in an oven at 32±2ºC with 200 mL of KCl solution (84% RH). After the specified interval, the patches were weighed () after 24 hours to calculate WVP according to the following equation:

$$P = \frac{Q \times D}{A \times T \times S \times (R_1 - R_2)} \times 100$$

Where; P is the permeability of patch (ng/s.m.Pa), Q is water absorbed (mg) by the patch at time T (h), d is the thickness of BF film (cm), A is the area of the film ($cm^2$), S is saturated vapor pressure at a specific temperature (Pa), $R_1$ is RH in the chamber (84%); and $R_2$ is RH inside the loaded-vial (0%) (12).

***In vitro permeability studies of BF transdermal patch***

The *in vitro* diffusion studies on BF transdermal patches were done across synthetic membrane (0.22 µm) using a Franz diffusion cell. For the preparation of the synthetic membrane, the membrane was soaked in PBS (pH 7.4) for 4 hours for equilibration. For each of the five transdermal patches (BO1 to BO5) (*n*=3), circular fragments were obtained and placed on the Franz diffusion cell with a diffusional area of 1.2 cm². The Franz diffusion cell consisted of two distinct chambers: the inner chamber to hold the diffusion medium and the synthetic membrane, and the outer chamber to regulate the water circulation to maintain the buffer temperature at 35±2°C. The inner chamber was filled with 12 mL phosphate buffer saline (PBS pH 7.4). After predetermined time, the buffer chamber was decanted and replaced with fresh buffer. The samples were collected for 24 hours and diluted with the suitable amount of buffer. Each sample collection was replicated thrice and subjected to UV/vis spectrophotometry analysis at 223 nm. The drug release was estimated with reference to the calibration curve, which was prepared with PBS pH 7.4 (y=0.0345x + 0.3475; R²:0.9962) using the stock solution dilution method in the concentration range of 1-32 µg/ml (13; 14).

***Ex vivo permeability studies of BF transdermal patch containing permeation enhancer***

The *ex vivo* diffusion studies on BF transdermal patches were done across rabbit skin using a Franz diffusion cell. For the preparation of rabbit skin, an electric shaver was used to remove hair from the dorsal skin, followed by the application of Veet hair removal cream. Afterwards, cream was removed from the skin surface with lukewarm water and washed thoroughly. The animals were left for 24 hours in animal house facilities. At the time of euthanization, the rabbits were anesthetized and sacrificed by cervical dislocation. The skin was carefully removed from the abdominal region and examined for surface integrity. Immediately afterwards, the skin was dipped in lukewarm water for 1 min to loosen the adhering fats. The skin was dabbed dry, and the dermis side was cleaned with an alcohol swab. Subsequently, the skin was washed with distilled water and stored in PBS (pH 7.4) buffer containing 0.02% sodium azide as a preservative and refrigerated at -20°C till further analysis (15).

In order to attain equilibrium throughout testing, the skin was first defrosted for ten hours in normal saline solution and then immersed for one hour in PBS (pH 7.4) (17). For each of the transdermal patches (*n*=3), circular discs were affixed to the rabbit skin with the stratum corneum facing the donor compartment of the Franz diffusion cell. The inner chamber was filled with 12 mL phosphate buffer saline (PBS pH 7.4), placed on a hot plate stirrer and agitated at 100 rpm for 24 hours to maintain sink conditions. A similar method was concurrently adopted for the placebo patches and BO1 as control systems to minimize the impact of any material leaking from the patch or skin. After predetermined time, the buffer chamber was decanted and replaced with fresh buffer. The samples were collected for 24 hours and diluted with the suitable amount of fresh buffer. Each sample collection was replicated thrice and subjected to UV/vis spectrophotometry analysis at 223 nm (13; 14).

Based on the optimal drug release patterns, the desired patch was further evaluated for an *ex vivo* study across the rabbit skin using permeation enhancer-loaded transdermal patch. The cumulative drug release (µg/cm²) was caculated with referernce to the calibration curve using the following formula:

$$Q = C_n \times V + \sum C_{n-1} \times V_n / M$$

Where, Q is the cumulative drug release (µg/cm²); is concentration at various time points (µg/mL); V is the volume of receiving solution (mL); and is the sampling volume (mL).

### *Microneedle-mediated transdermal delivery of BF transdermal patch*

Stainless steel microneedles were used for the microneedle-mediated transdermal delivery of BF using an optimized formulation based on *ex vivo* experiments. The microneedles were manually rolled and pressed into the excised skin. The perforated skin was then mounted on the Franz diffusion cell and clamped between the receptor and donor compartments as described previously.

### *Kinetics model and flux of BF transdermal patch*

At the end of the *ex vivo* studies, the skin surface exposed to the BF film was examined for any evident redness or abnormalities and compared to the control patch skin. The amount of BF penetrated per unit area of rabbit skin (**µg**/cm²) was quantified and plotted with time. The steady-state flux (Jss) was computed as **µg**/cm²/min by dividing the slope of the linear portion of the curve over the area of the exposed skin surface (1.2 cm²). Also, the enhancement ratio (ER) was calculated by dividing the flux obtained after permeation enhancer addition by the flux obtained without permeation enhancer.

Additionally, the *ex vivo* permeation data was analysed with kinetic models using DDSolver, including zero order, first order, Higuchi model, and Korsmeyer-Peppas (KP) model (16).

### *Skin irritancy test for BF transdermal patch*

The susceptibility of the transdermal patch to cause skin irritancy was observed as per the guidelines of the Draize method. The trials were carried out under controlled conditions at animal house facilities provided by the Faculty of Pharmacy, The University of Lahore, Lahore, Pakistan. Two groups were formed for rabbits, one as a control and the other to test the patch. The skin irritancy test was classified using a visual scoring system, with '0' indicating no irritation, '1' indicating minimal irritation, '2' indicating well-defined skin irritation, '3' indicating significant irritation, and '4' representing scar development (17).

### *Thermal analysis of the optimized formulation*

Differential scanning calorimetry (DSC) and thermogravimetric analysis (TGA) studies were performed on Eudragit L-100, HPMC, PEG 400, and permeation enhancer along with the optimized formulation of the BF transdermal patch. For DSC analysis, the samples were analyzed on TA instruments Q2000 series Thermal Analysis System (TA instruments, UK) within a thermal range of 20-300°C at a scan rate of 10°C/min. For the TGA analysis, the samples were assessed in the range of 2 theta with the scan speed of 10º/min uaing TA instruments Q5000 series Thermal Analysis System. The system was operated in the temperature range of 25-500℃, while keeping the current and voltage to 22 mA and 30kV, respectively.

### *Stability studies for transdermal patch of Bisoprolol fumurate*

Preliminary physicochemical stability of the optimized formulation was evaluated by storing the BF transdermal patches at accelerated conditions of 25±2 ℃ (60±5% RH) and 40±2 ℃ (75±5% RH) for 168 days. The patches were taken out at predetermined intervals of 7, 28, 84, and 128 days. Any changed in the organoleptic characteristics, thickness, weight, and drug content was recorded.

## Results and discussion

### *Organoleptic properties of BF transdermal patch*

In the present study, different matrix-type transdermal patches of BF were prepared to assess the percutaneous penetration of the drug across the excised skin. In addition to the drug release pattern, the organoleptic properties of the patch are a desirable characteristic to select the most appropriate choice of

polymeric blend and permeation enhancer. The formulated patches (BO1 to BO5) were prepared using different concentrations of HPMC and Eudragit L-100 with a fixed concentration of BF. The prepared transdermal patches were subjected to various visual inspection parameters to ensure uniform polymer and drug distribution in the matrix system. Based on organoleptic characteristics, Table 2, BO1 and BO2 had a slightly opaque color mainly because of the presence of a higher concentration of HPMC. A similar observation has been reported previously that HPMC forms a slightly opalescent solution (18). On the flip side, transdermal patches containing a higher concentration of Eudragit L-100 gave a clear and colorless solution. BO3, BO4, and BO5 had a glossier appearance as compared to other formulations. Gloss is an optical property which is based on the interaction of light with the physical characteristic of a polymeric surface. The prepared patches had a smooth surface and the flexibility of the patch tended to improve with an increase in Eudragit L-100 concentration. The matrix system was homogenous, and the patches complied with the desired specifications.

Table 2: Organoleptic properties of Bisoprolol transdermal patch

| Formulation | Translucency | Transparency | Gloss | Smoothness | Flexibility | Homogeneity |
|---|---|---|---|---|---|---|
| BO1 | ++ | ++ | ++ | +++ | ++ | +++ |
| BO2 | ++ | ++ | ++ | +++ | ++ | +++ |
| BO3 | + | +++ | +++ | +++ | ++ | +++ |
| BO4 | + | +++ | +++ | +++ | +++ | +++ |
| BO5 | + | +++ | +++ | +++ | +++ | +++ |
| BO1-S9 | + | ++ | + | ++ | +++ | ++ |
| BO1-S12 | + | +++ | ++ | +++ | +++ | +++ |
| BO1-O9 | + | +++ | ++ | +++ | +++ | +++ |
| BO1-O12 | ++ | ++ | +++ | ++ | +++ | ++ |
| BO1-A9 | + | +++ | ++ | +++ | +++ | +++ |
| BO1-A12 | + | ++ | ++ | ++ | ++ | ++ |

` The patches containing higher concentratin of oleic acid were slightly translucent as compared to the other patches, possibly due to crystallization of BF. A higher drug load in the transdermal patch promotes higher flux; however, sometimes crystal formation may occur due to metastablity and thermodynamic activity (19). The presence of dispersed surfactant aggregates enhances light scattering, therefore BO1-O12 appeared more glossier than the rest. In addition, the patches containing higher concentrations of oleic acid and orange oil had comparatively less homogeneity and surface smoothness as compared to Span 20 patches and BO1-O9 and BO1-A9 (20).

***Physicochemical evaluation of BF transdermal patch***

As seen in Figure 1 (A), the weight of the patches ranged from 960±41 mg to 890±32 mg. An increased weight was observed in BO1, containing the highest concentration of HPMC, possibly due to the moisture-absorbing nature of HPMC. The result was backed up by the thickness and moisture uptake studies on the transdermal patches. As seen in Figure 1 (B), the highest thickness of 0.51±0.32 mm was estimated for BO1, whereas BO5 had the least thickness of 2.28±0.79 mm. In the case of

patches containing permeation enhancer, an increase in weight was observed as compared to the parent patch BO1. As observed in Figure 1 (A), BO1-O9 and BO1-O12, containing orange oil, had slightly more weight than the other formulations. This could be due to the less hydrophobic properties of orange oil compared to Span 20 and oleic acid. Additionally, adding propylene glycol to orange oil has been shown to slightly improve the miscibility of d-limonene (21). Also, the addition of permeation enhancer tended to increase the thickness of the patch, as seen in Figure 1 (B). Based on the results, BO1-A12, containing 12% w/w of oleic acid, yielded the thickest films. It has been previously reported by Fadilah *et al.* (2024) that the addition of Tween 80 with PEG 400 increases the thickness of the patch to a greater extent (22). A similar conclusion can thus be formed for oleic acid, as Tween 80 is a complex nonionic surfactant that includes oleic acid as one of its components.

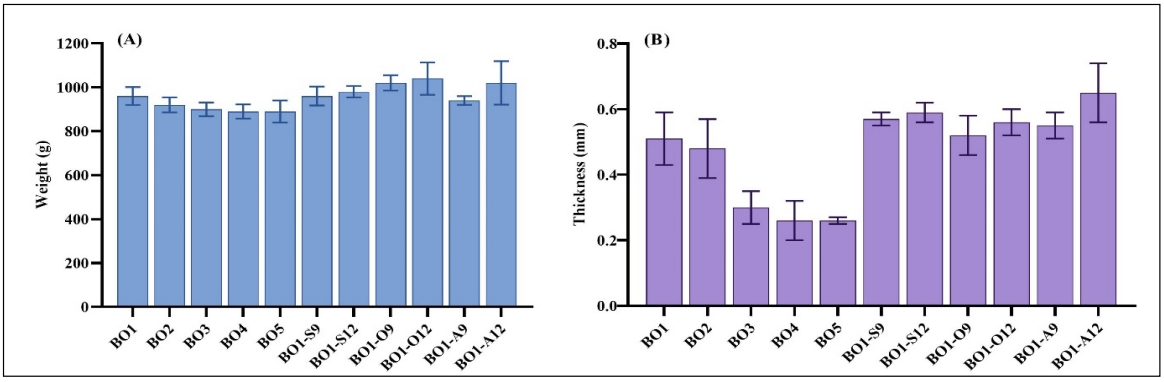


Figure 1: (A) Weight and (B) thickness of BF transdermal patch without (BO1 to BO5) and with (BO1-S9 to BO1-A12) permeation enhancers

The drug content in the films was in the range of 94.55±0.38% to 99.12±0.53%, which complied with official limits (85-115%) of USP-NF. The uniform drug content and minimum drug variability within the different batches ensure the homogenous dispersion of the drug in the matrix-type BF transdermal patch.

### *Moisture analysis of BF transdermal patch*

As shown in Figure 2, the moisture content of the BF transdermal patches ranged between 1.78-4.22%. In the case of moisture content of the transdermal patch without permeation enhancer, the formulation BO1 containing a higher amount of HPMC resulted in an increased retention of moisture content after drying. The result was supported by data on weight analysis and thickness. Due to the hydrophilic nature of HPMC, the polymer can absorb and retain water from the environment in its structure due to hydrogen bonding. The number of functional groups that can form bonds with water molecules from the environment governs the degree of moisture absorption (23). HPMC contains several polar functional groups in its structure, including hydroxyl groups, hydroxypropyl groups, and methoxyl groups. These polar groups are attracted to moisture present in the environment, forming a hydrated layer on the polymer's surface. The attractive forces between the polymer and water facilitate the diffusion of water molecules into the polymer structure. These hydrogen bonds are relatively weak and primarily exist between the hydrogen atom of the water molecule and the nitrogen and/or oxygen atom of the polymer (24). On the flip side, the formulation BO5 containing the higher amount of Eudragit L-100 resulted in the least moisture content after drying. As Eudragit L-100 contains more hydrophobic regions, it has the least tendency to absorb and retain water in its structure. While moisture content is beneficial

in certain cases, especially prevention of brittleness, it can also lead to other issues such as bulkiness, drug release rate, microbial contamination, and flexibility. The studies have demonstrated that a moisture content within the range of 2-10% is generally desirable while retaining the mechanical strength and stability (12).

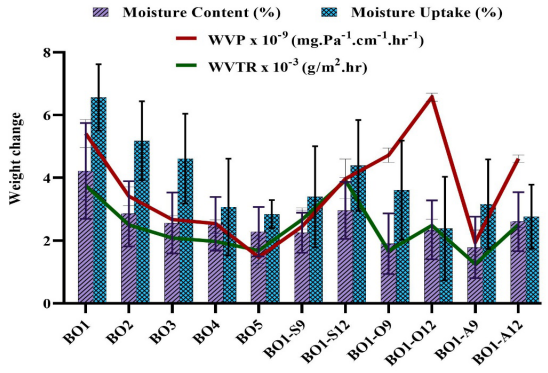


Figure 2: Moisture analysis of BF transdermal patch with and without permeation enhancers

As per analysis, the moisture content was less than 2% in BO1-O9 and BO1-A9, containing orange oil and oleic acid, respectively. Oleic acid is a monounsaturated fatty acid with a hydrophilic carboxylic acid head but a long hydrophobic hydrocarbon tail in its structure. Also, the HLB value of oleic acid is approximately 1.0, making it a highly lipophilic compound (25). Similarly, orange oil is primarily composed of D-limonene, which is a cyclic monoterpene hydrocarbon containing no polar hydrophilic group (26). On the other hand, Span 20 contains multiple -OH groups from sorbitol (sugar alcohol) and has an HBL value of 8.6 (27). Hence, Span 20 is more hydrophilic among the three permeation enhancers due to sugar-derived polyol headgroups present in its structure. Thus, the moisture content was slightly higher in Span 20 BF transdermal patches (BO1-S12; 2.96%) as compared to other formulations with permeation enhancers.

In the case of moisture uptake studies, an increased drift in moisture was observed at 84% RH, as seen in Figure 2. The moisture uptake ranged between 2.84-6.56% and 2.38-4.39% in patches with and without permeation enhancers, respectively. Similar to moisture content, the highest moisture uptake tendency was depicted by BO1 and BO1-S12 as compared to the other formulations. It has been previously reported that moisture uptake of less than 15% w/w prevents bulkiness of the patch (12). Hence, the patches complied with the specifications for moisture content and moisture uptake.

### *WVTR estimation in Bisoprolol fumarate transdermal patch*

To ensure the stability of the patch during storage conditions, WVTR was calculated to estimate how much water vapor may pass through it over time. In addition to the hydration potential of the skin, WVTR is influenced by the moisture balance in the formulation. As shown in Figure 2, BO1 showed a maximum WVTR of 3.75×10-3 g/m²/h due to higher content of hydrophilic polymer. HPMC has a tendency to form a gel barrier, which can initially slow the rate of vapor transmission. However, WVTR increases over time due to swelling and increased moisture diffusion across the HPMC. The formulation BO5 showed a minimum WVTR of 1.68×10-3 g/m².h. Despite having the highest concentration of Eurdagit L-100, BO5 was able to transmit vapor and absorb moisture due to the presence of PEG 400 as a plasticizer. PEG 400 is a hydrophilic and hygroscopic polymer that enhances the free volume and pore channels, allowing moisture to move through more easily in the transdermal patch. Despite the variations, the low level of WVTR is an indication of good stability and ensures long-term storage of the transdermal patch (28).

The lowest WVTR for transdermal patches containing permeation enhancers was 1.25×10-4 g/m².h (BO1-A9), while the highest was 3.92×10-4 g/m².h (BO1-S12). The findings were consistent with previous moisture content and moisture uptake results of BF transdermal patches. At greater concentrations, Span 20 may plasticize the matrix system, increasing

free volume and slightly raising the WVTR (29). In comparison to BO1, transdermal patches containing oleic acid (lipophilic fatty acid) and orange oil (nonpolar essential oil) showed reduced WVTR, owing to the occlusive nature of these permeation enhancers (30).

WVP measures the permeability coefficient of transdermal patch, combining diffusion and solubility. In practice, WVTR gives an insight into the storage stability, whereas WVP also predicts the dissolution profile. BO1 showed maximum vapor permeability with the value of $5.41\times10^{-9}$ ($mg.Pa^{-1}.cm^{-1}.hr^{-1}$) due to the hydrophilic nature of HPMC. The minimum WVP value was $1.36\times10^{-9}$ ($mg.Pa^{-1}.cm^{-1}.hr^{-1}$) for BO5 because of the hydrophobic nature of Eudragit L-100. The WVP ranged from $1.92\times10^{-9}$ $mg.Pa^{-1}.cm^{-1}.hr^{-1}$ to $6.57\times10^{-9}$ ($mg.Pa^{-1}.cm^{-1}.hr^{-1}$) in BF transdermal patches with permeation enhancers.

***In vitro permeability studies of BF transdermal patch without permeation enhancer***

The *in vitro* dissolution studies were carried out on Franz diffusion through the synthetic membrane for 24 hours to select an optimized patch for the loading of permeation enhancer. As presented in Figure 3, the maximum drug release was observed in BO1, mainly due to the high permeability of HPMC to buffer, which results in a decreased diffusional path length for drug release. The formulation released 6864.17 µg/cm² (equivalent to 8237.0 µg) of drug in 24 hours. The minimum drug release was observed in BO5 because of the higher amount of Eudragit L-100. Unlike HPMC, Eudragit L-100 is much less water soluble and less swellable in PBS (pH 7.4) buffer. This hydrophobic polymer does not readily absorb aqueous fluid when the transdermal patch comes in contact with the skin or dissolution medium. Low polymer swelling is a critical parameter in transdermal formation because swelling opens pores and increases the diffusional pathways for drug movement.

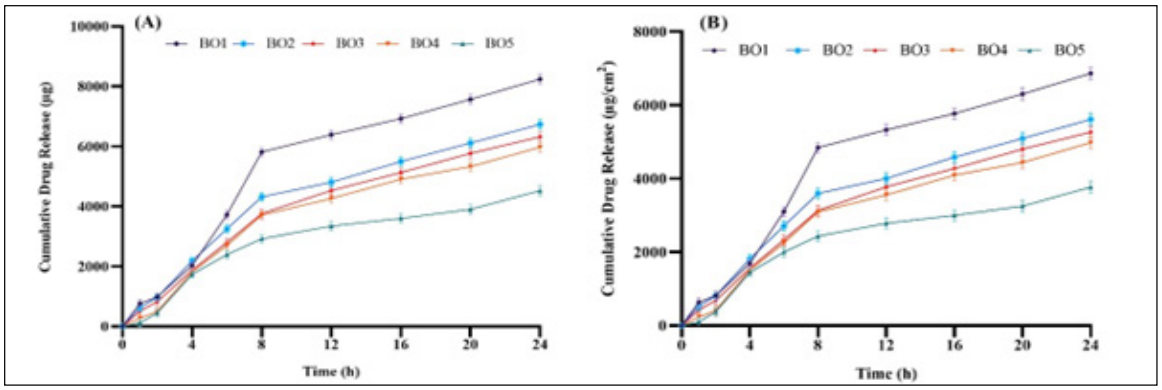


Figure 3: *In vitro* drug release pattern of BF from transdermal patch across synthetic membrane

As seen in Table 3, 25% of the drug was released from BO1 within 3.8 hours, whereas 50% of the drug release was obtained within 12 hours. Other formulations required more than 18 hours for 50% of drug release. In addition, 75% of the drug was released in 22.82 hours. The results confirms the sustained and desired rate of drug release from the transdermal patch BO1. The addition of Eudragit L-100 in the formulation retarded the drug release, where 67.29% (equivalent to 5607.5 µg/cm² and 6729 µg) of BF was released after 24 hours. The release was reduced to 45.21% (3767.5 µg/cm² and 4521.0 µg) when the transdermal patch was composed entirely of Eudragit L100 as a polymer in BO5. According to kinetic models, Table 4, the formulations followed the Higuchi model which signifies that the release of the

drug was diffusion controlled. The drug release mechanism was further verified through the KP model which indicated that BO1-B03 had an n value greater than 0.45. This signifies that the BF release was greatly controlled by diffusion and swelling mechanisms (31). The results are in good agreement with the swelling behavior of HPMC. As the concentration of Eudragit L100 increased in BO4 and BO5, the drug release mechanism became diffusion controlled. Based on these findings, the formulation BO1 was chosen as the optimal formulation for the addition of permeation enhancers.

Table 3: Predicted *in vitro* pattern for 25%, 50%, 75%, and 80% BF release from transdermal patch

| Parameter | BO1 | BO2 | BO3 | BO4 | BO5 |
|---|---|---|---|---|---|
| $t_{25\%}$ | 3.818 | 5.375 | 6.513 | 7.163 | 10.890 |
| $t_{50\%}$ | 12.496 | 18.838 | 21.102 | 23.172 | 39.091 |
| $t_{75\%}$ | 26.961 | 41.276 | 45.419 | 49.855 | 86.093 |
| $t_{80\%}$ | 30.548 | 46.841 | 51.449 | 56.472 | 97.749 |

Table 4: *In vitro* kinetic model for BF transdermal patches across synthetic membrane

| Formulation | Zero Order ($R^2$) | First Order ($R^2$) | Higuchi ($R^2$) | KP ($R^2$) | n |
|---|---|---|---|---|---|
| BO1 | 0.8775 | 0.9358 | 0.9535 | 0.9489 | 0.538 |
| BO2 | 0.9049 | 0.9589 | 0.9847 | 0.9827 | 0.514 |
| BO3 | 0.9264 | 0.9711 | 0.9891 | 0.9872 | 0.557 |
| BO4 | 0.9062 | 0.9529 | 0.9897 | 0.9910 | 0.450 |
| BO5 | 0.8574 | 0.8957 | 0.9751 | 0.9935 | 0.361 |

***Ex vivo permeability studies of BF transdermal patch with permeation enhancer***

As seen in Figure 4, the cumulative drug release (µg/cm²) tended to increase with an increase in concentration of Span 20, orange oil, and oleic acid in BO1-S12, BO1-O12, and BO1-A12, respectively. The release curves mainly consisted of two phases; in the first phase a burst release is observed, and then 'slow-release' occurs in the second phase. The initial burst release is beneficial for the rapid drug availability at the target site. For a uniform

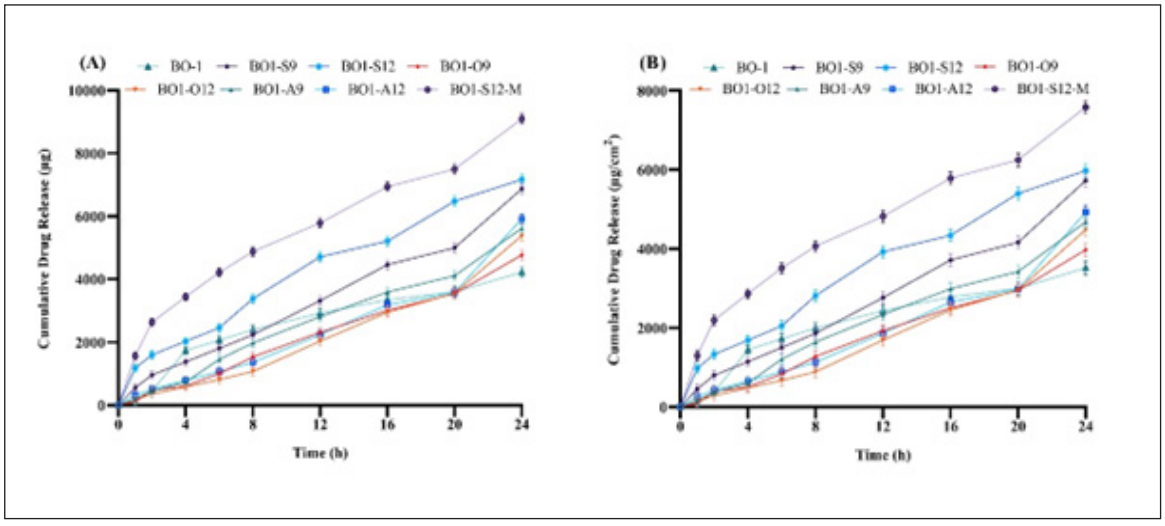


Figure 4: *Ex vivo* drug release pattern of BF from transdermal patch containing permeation enhancers across excised rabbit skin

drug release over 24 hours, it is necessary that 50% of the drug should be released in 12 hours. Based on these assumptions, highest drug permeation across the rabbit skin was obtained in BO1-S12, which corresponded to 4707.6 µg or 3923.0 µg/cm² of BF in 12 hours. On the other hand, BO1-O12 showed a drug release of 2029.2 µg (corresponding to 1691.0 µg/cm²), whereas BO1-A12 showed a slightly higher drug release of 1867.2 µg (corresponding to 2240.8 µg/cm²) after 12 hours. However, the results were not significantly different from one another ($p$>0.05). By the end of 24 hours, BO1-S12 had release 71.68% of the drug, Figure 4, whereas 53.82% and 59.12% of the drug released from BO1-O12 and BO1-A12, respectively. These results signify that amongst the three permeation enhancers, Span 20 has the greatest tendency to aid the permeation of BF across the stratum corneum.

The release curves were also subjected to kinetic models, including zero order, first order, the Higuchi model, and the KP model. The cumulative percentage of drug release versus time showed that the drug release from BO1-S12 followed the Higuchi model, Table 5. According to the KP model, the value of n was greater than 0.45; therefore, the BF release mechanism was a combination of swelling and diffusion procedures. As a general conclusion, irrespective of the solubility, the release of BF was mainly controlled by the polymers.

Table 5: *Ex vivo* kinetics models, flux (**µg**/cm²/h), and ER for BF transdermal patch across rabbit skin

| | Zero Order ($R^2$) | First Order ($R^2$) | Higuchi ($R^2$) | KP ($R^2$) | n | Flux (µg/cm²/h) | ER |
|---|---|---|---|---|---|---|---|
| BO1 | 0.8899 | 0.7526 | 0.9857 | 0.9811 | 0.496 | 118.03 | N/A |
| BO1-S9 | 0.9880 | 0.9737 | 0.9218 | 0.9865 | 1.04 | 181.92 | 1.54 |
| BO1-S12 | 0.9722 | 0.9663 | 0.9869 | 0.9890 | 0.68 | 195.11 | 1.65 |
| BO1-O9 | 0.9923 | 0.9845 | 0.9491 | 0.9919 | 1.07 | 134.00 | 1.14 |
| BO1-O12 | 0.9640 | 0.9373 | 0.9081 | 0.9890 | 1.76 | 144.14 | 1.22 |
| BO1-A9 | 0.9901 | 0.9844 | 0.9606 | 0.9888 | 0.97 | 156.00 | 1.32 |
| BO1-A12 | 0.9505 | 0.9231 | 0.8752 | 0.9721 | 2.11 | 150.25 | 1.27 |
| BO1-S12-M | 0.9278 | 0.9666 | 0.9919 | 0.9914 | 0.52 | 225.67 | 1.91 |

Span 20, a nonionic surfactant, has the potential to penetrate the intracellular portion of the stratum corneum. Once inside, it increases the fluidity or may remove lipid components. Afterwards, Span 20 moves into the intracellular matrix and binds with the keratin filaments, disrupting the corneocytes. These alterations in the stratum corneum eventually allow the transport of the drug across the membrane. In addition, the enhancement of the cutaneous absorption is linked with the high solubility of BF in the transdermal patch. The high recovery rate of the drug along with the larger surface area of the transdermal patch supports the interaction of Span 20 with the stratum corneum. Orange oil is a rich source of terpenes, having d-limonene as the major constituent (32). Terpene contains a functional group that tends to donate or accept hydrogen bonds, intitiating the loosening of the interlamellar hydrogen bonding within the lipid bilayer, and hence forming new polar channels which increases the permeability of BF.(33) In the case of oleic acid, it is reported that this permeation enhancer reduces the diffusional resistance by interacting with the lipid matrix within the skin and by increasing lipid fluidity. Another suggested mechanism of oleic acid is lamellar solid-fluid phase separation and lipid extraction of the stratum corneum (34).

***Flux of BF transdermal patch containing permeation enhancer***

As evident from Table 5, the flux of the patches containing permeation enhancers was greater than the control patch. The highest flux was achieved by BO1-S12, followed by BO1-S9. Interestingly, the flux and ER of BO1-A9 (flux: 156.00 µg/cm²/h, ER: 1.32) were greater than those of BO1-A12 (flux: 150.25 µg/cm²/h, ER: 1.27). Similar outcomes have been documented in the previous literature, where a distinct phase emerges within the stratum corneum lipids due to an elevated concentration of oleic acid. Therefore, it doesn't further alter the endogenous lipid domain, which would affect the rate of drug release over time (35).

***Effect of microneedle on permeation of BF***

Before the application of microneedles on excised rabbit skin, the transepidermal water loss (TEWL) was measured to verify the integrity of the skin barrier. A lower TEWL value (9.85±2.65 g/m².h.) confirmed the structural integrity of the stratum corneum, whereas a higher TEWL value (34.17±1.95 g/m².h.) indicated the formation of micropores after microneedle treatment. As seen in Figure 4, a drastic increase in cumulative permeation of BF (9096.0 µg or 7580 µg/cm²) was observed when BO1-S12 was applied on microneedle-treated skin. The formulation followed the Higuchi model with an anomalous drug release mechanism. With this pretreatment approach, the formation of the micropores in the stratum corneum allows the diffusion of BF across the dermis into the systemic circulation. As indicated in Table 5, BF flux was significantly higher through microneedle-treated skin ($p$<0.05) as compared to BO1-S12. The increase in flux after microneedle treatment was expected, since these tiny projections disrupt the skin barrier function and increase permeability of hydrophilic drugs like BF. This also means that a threshold had been surpassed at which a high concentration of Span 20 at 12% w/w was able to assist the permeation of 90.96% of BF for 24 hours when combined with the micropore channel pathway. Our studies have previously reported the use of dissolving microneedles as a pretreatment approach for the promising delivery of hydrophilic drug Acyclovir (36) and hydrophobic drug Diacerein (37; 38).

***Skin irritation test for optimized formulation BO1-S12***

The skin irritation or sensitization test was conducted on rabbits and assessed by the Draize method. As indicated in Table 6, the animals showed only a slight irritation in the first hour of microneedle application, whereas the erythema completely subsided after 24 hours. In the case of transdermal patch alone, there was no sign or erythema or redness after 1 hours or 24 hours. The results indicate that the microneedles and BO1-S12 were safer to wear for a prolonged time and did not cause any permanent alterations on the skin.

Table 6: Grading for skin sensitization potential after the removal of BF transdermal patch (BO1-S12) and microneedle application

| Time | 1 hour | 24 hours |
|---|---|---|
| BO1-S12 | 0 | 0 |
| BO1-S12-M | 1 | 1 |

***Stability studies of optimized BF transdermal patch***

The transdermal films were analyzed at 0 days, 1, 2, and 3 months as per ICH guidelinesand the results are given in Table 7. The accelerated stability studies indicated that no major changes occurred in the weight, drug content, and thickness of the patch. There was no evident change in color, flexibility, or integrity of the patch. The drug content remained within the official limitation prescribed by USP-NF.

***Thermal analysis of the optimized formulation***

The thermal analysis of the drug, polymers, and permeation enhancer of the optimized formulation of given in Figure 5. As seen in DSC traces of crystalline BF, the first heating

Current Trends in Biotechnology and Pharmacy
Vol. 19(4) 2603-2620, October 2025, ISSN 0973-8916 (Print), 2230-7303 (Online)
DOI: 10.5530/ctbp.2025.4.41


phase showed one endothermic peak at 95.5℃ due to the loss of water or possible melting of BF. Another sharp endothermic peak was evident at 101.4℃ due to melting of the drug. The presence of nanocrystalline domains in the crystalline sample can lower the peak of melting (39). A broad endothermic peak was obtained for HPMC, whereas the exothermic peak started near 210℃ (36). Eudragit L100 displayed sharp endothermic peaks near 70℃and a very slight dip near 210℃. The first peak was side chain mobility (β-relaxation), whereas the second dip was due to anhydride formation during water evaporation. A sharp downward peak in the region of 380–420°C corresponded to the polymer degradation.(40) For Span 20, the DSC data showed a broad endothermic peak between 60 and 75℃ which denotes the melting point temperature of the liquid. As the temperature increased from 100 to 300°C, the curve was exothermic and corresponded to two concomitant weight change steps. The first phase between 100 and 200℃ can be described as the initiation of the autoxidation process. In this process the insertion of oxygen causes a chain-breaking reaction that leads to the formation of primary oxidation products. In the second exothermic event, secondary degradation occurs between 200 and 300℃. A sharp decline between 310 and 360℃ represents the complete breakdown of the primary polymer (41). The DSC curve of the physical mixture, Figure 6, did not show any overlapping or broad endothermic peaks, suggesting that no interaction occurred between the drug, polymer, and the permeation enhancer.

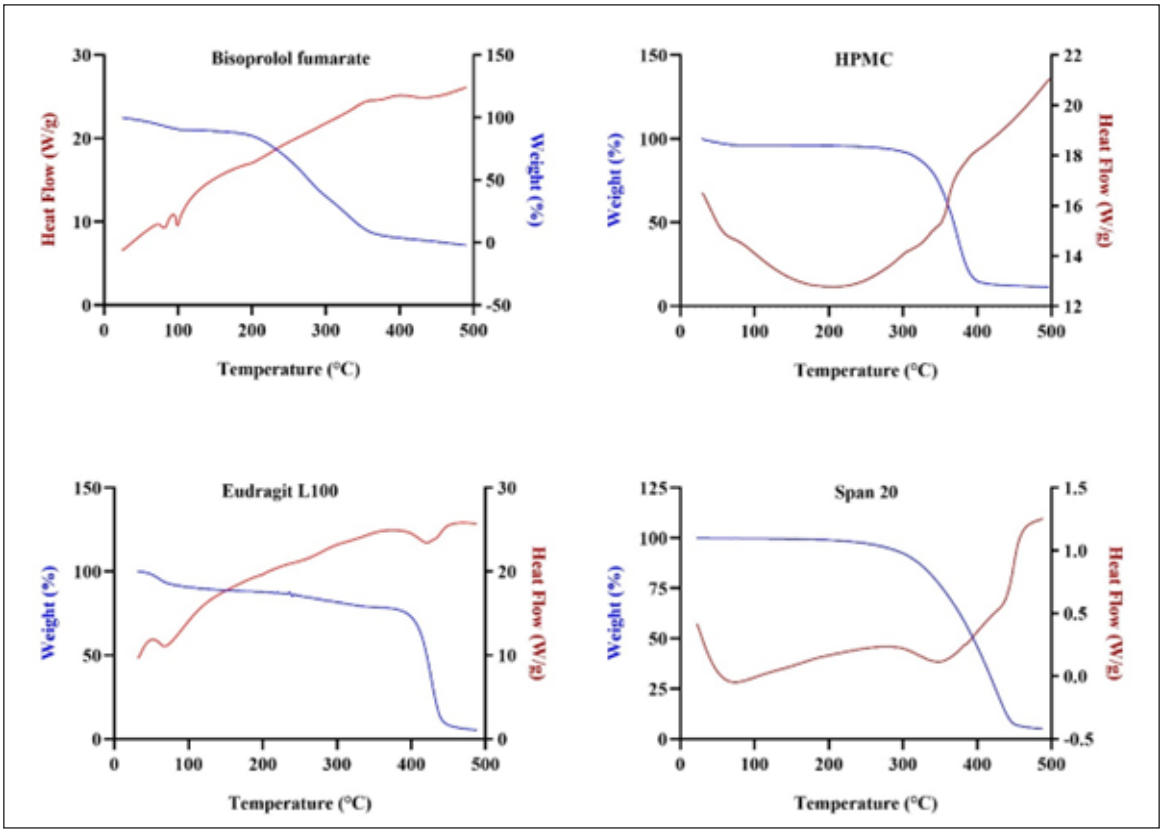


Figure 5: Thermal analysis of drug (BF), polymers (HPMC and Eudragit L100), and permeation enhancer (Span 20)

In the TGA graph, a slight change in weight near 60-100℃ can be attributed to the moisture loss. However, a sharp weight loss, corresponding to a 78.79% weight difference, between 250 and 370°C can be attributed to the decomposition of the drug. The TGA graph of HPMC showed a slight weight loss between 90 and 100°C that indicated the water loss from the polymer. A single-step degradation was evident between 240 and 400℃ that corresponded to a total weight loss of 80% (36). The TGA curve of Eudragit L100 indicated approximately 5% weight loss between 70 and 100℃ due to the release of surface water (42). The total weight of 67% was observed in the temperature range of 400-450℃, mainly because of the decomposition of the polymer.In the TGA analysis of Span 20, the onset of weight loss was pushed to a higher temperature of approximately 280℃ The weight loss of 87.68% was recorded between 280 and 450℃ for Span 20. According to Kishore *et al.* (2011), the changes in TGA begin only when volatile degradants are formed and radical formation occurs at the olefinic and polyoxyethylene sites of Span 20 (41). The TGA curve of the physical mixture, Figure 6, did not show any abnormal weight losses, suggesting that no interaction occurred between the drug, polymer, and the permeation enhancer.

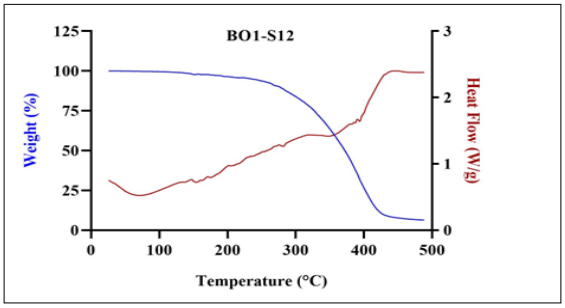


Figure 6: Thermal analysis of the optimized formulation BO1-S12

## Conclusion

Presently, we have demonstrated the potential use of permeation enhancers in a transdermal patch of BF using HPMC: Eudragit L-100 (5:1) with 40% w/w PEG 400 as a plasticizer. In addition to the formulation optimization, the use of solid microneedles as a pretreatment strategy to enhance drug permeation and retention for 24 hours is also demonstrated. As per in vitro analysis across a synthetic membrane, the higher concentration of HPMC with a lower concentration of Eudragit L100 successfully controlled the release of BF for 24 hours. When the patch (HPMC: Eudragit 5:1) was loaded with permeation enhancers, including Span 20, orange oil, and oleic acid, the disruption of stratum corneum was confirmed due to the evident increase in cumulative drug permeation across the excised rabbit skin. However, the result was not pronounced as expected with oleic acid and orange; however, Span 20 at 12% w/w concentration allowed 71.68% of BF release in 24 hours. Therefore, pretreatment of skin with solid microneedles was undertaken to form micropores and hydrophilic pathways for drug permeation and skin saturation. This approach effectively increased the cumulative BF permeation and delivered up to 90.96% of the drug. To reduce the chances of contamination and ease of application, polymeric microneedles can also be used instead of solid microneedles. While the purpose of the present study was the development and optimization of a BF-loaded transdermal patch, further in vivo studies will help confirm the BF plasma concentrations within the therapeutic window for a prolonged time period. Strategically optimizing the combined effect of microneedles and permeation enhancers could further reduce the patch size, increasing patient compliance and discretion.

## Acknowledgements

Declared none.

## Competing interests

The authors have no relevant financial or non-financial interests to disclose.

## Funding

The authors declare that no funds, grants, or other support were received during the preparation of this manuscript.

**Authors' contributions**

**AA:** data collection and processing, analysis and interpretation, literature search, writing; **MS and UN:** concept, design, analysis and interpretation, approval for the final draft; **AAB:** writing and interpretation; **AM, AF, SA:** data collection and processing, literature search, and writing, **MAA, MAKS, MAUK:** data collection and processing and literature search.

**References**

1. Ahad, A., Al-Jenoobi, F. I., Al-Mohizea, A. M., Akhtar, N., Raish, M., & Aqil, M. (2015). Systemic delivery of β-blockers via transdermal route for hypertension. *Saudi Pharmaceutical Journal*, *23*(6), 587-602.
2. Organization, W. H. (2023). *Global report on hypertension: the race against a silent killer*. World Health Organization.
3. Shafi, S. T., & Shafi, T. (2017). A survey of hypertension prevalence, awareness, treatment, and control in health screening camps of rural central Punjab, Pakistan. *Journal of epidemiology and global health*, *7*(2), 135-140.
4. Sinnott, S.-J., Douglas, I. J., Smeeth, L., Williamson, E., & Tomlinson, L. A. (2020). First line drug treatment for hypertension and reductions in blood pressure according to age and ethnicity: cohort study in UK primary care. *bmj*, *371*.
5. Ansari, K., Singhai, A., & Saraogi, G. K. (2011). Recent advancement in transdermal drug delivery system. *Int J Pharm Pharm Sci*, *3*(5), 52-59.
6. Momomura, S.-i., Saito, Y., Yasumura, Y., Yamamoto, K., Sakata, Y., Daimon, M., Kinugawa, K., Okamoto, H., Dohi, N., & Komuro, I. (2017). Efficacy and Safety of Switching From Oral Bisoprolol to Transdermal Patch in Japanese Patients With Chronic Heart Failure. *Circulation Journal*, CJ-17-0532.
7. Yamashita, T., Ikeda, T., & Akita, Y. (2019). Comparison of heart rate reduction effect and safety between bisoprolol transdermal patch and bisoprolol fumarate oral formulation in Japanese patients with persistent/permanent atrial fibrillation (BISONO-AF study). *Journal of Cardiology*, *73*(5), 386-393.
8. Song, W., Cun, D., Xi, H., & Fang, L. (2012). The control of skin-permeating rate of bisoprolol by ion-pair strategy for long-acting transdermal patches. *AAPS PharmSciTech*, *13*(3), 811-815.
9. Shabbir, M., Ali, S., Farooq, M., Adnan, S., Yousaf, M., Idrees, A., Rehman, K., & Shahid, N. (2016). Formulation factors affecting in vitro and ex vivo permeation of bisoprolol fumarate from a matrix transdermal patch. *Advances in Polymer Technology*, *35*(3), 237-247.
10. Kshirsagar, S. J., Bhalekar, M. R., & Mohapatra, S. K. (2012). Development and evaluation of carvedilol-loaded transdermal drug delivery system: in-vitro and in-vivo characterization study. *Drug development and industrial pharmacy*, *38*(12), 1530-1537.
11. Patel, R. P., Gaiakwad, D. R., & Patel, N. A. (2014). Formulation, optimization, and evaluation of a transdermal patch of heparin sodium. *Drug discoveries & therapeutics*, *8*(4), 185-193.
12. Shabbir, M., Fazli, A. R., Ali, S., Raza, M., Sharif, A., Akhtar, M. F., Ahmed, S., Peerzada, S., Younas, N., & Manzoor, I. (2017). Effect of hydrophilic and hydrophobic polymer on in vitro dissolution and permeation of Bisoprolol fumarate through transdermal patch. *Acta Poloniae Pharmaceutica*, *74*(1), 187-197.
13. Ham, A. S., Lustig, W., Yang, L., Boczar, A., Buckheit, K. W., & Buckheit Jr, R. W. (2013). In vitro and ex vivo evaluations on transdermal delivery of the HIV inhibitor

IQP-0410. *PloS one*, *8*(9), e75306.

14. Jafri, I., Shoaib, M. H., Yousuf, R. I., & Ali, F. R. (2019). Effect of permeation enhancers on in vitro release and transdermal delivery of lamotrigine from Eudragit® RS100 polymer matrix-type drug in adhesive patches. *Progress in biomaterials*, *8*(2), 91-100.
15. Ramadan, E., Borg, T., Abdelghani, G., & Saleh, N. (2018). Design and in vivo pharmacokinetic study of a newly developed lamivudine transdermal patch. *Future Journal of Pharmaceutical Sciences*, *4*(2), 166-174.
16. Costa, P., & Lobo, J. M. S. (2001). Modeling and comparison of dissolution profiles. *European journal of pharmaceutical sciences*, *13*(2), 123-133.
17. Khan, I., Anwar, N., Khan, M. S., Yadav, D. K., Shamsi, S., & Shamsi, A. (2024). In vitro and Ex vivo study targeting the development of a Lavandula stoechas L.(Ustukhuddūs) loaded Unani Transdermal patch: Implication of Unani Medicine in the treatment of Nisyan (Dementia). *Heliyon*, *10*(3).
18. Yi, T., Wan, J., Xu, H., & Yang, X. (2008). Controlled poorly soluble drug release from solid self-microemulsifying formulations with high viscosity hydroxypropylmethylcellulose. *European journal of pharmaceutical sciences*, *34*(4), 274-280.
19. Otterbach, A., & Lamprecht, A. (2021). Enhanced skin permeation of estradiol by dimethyl sulfoxide containing transdermal patches. *Pharmaceutics*, *13*(3), 320.
20. Chen, G., Zhang, B., & Zhao, J. (2015). Dispersion process and effect of oleic acid on properties of cellulose sulfate-oleic acid composite film. *Materials*, *8*(5), 2346-2360.
21. Yotsawimonwat, S., Okonoki, S., Krauel, K., Sirithunyalug, J., Sirithunyalug, B., & Rades, T. (2006). Characterisation of microemulsions containing orange oil with water and propylene glycol as hydrophilic components. *Die Pharmazie-An International Journal of Pharmaceutical Sciences*, *61*(11), 920-926.
22. Fadilah, N. A., Wahyuningsih, I., & Widyaningsih, W. (2024). In-vivo study of oleic acid and tween-80 on patch transdermal A. paniculata as anti-diabetic.
23. Ahmed, E. M. (2015). Hydrogel: Preparation, characterization, and applications: A review. *Journal of advanced research*, *6*(2), 105-121.
24. Bayliss, N., & Schmidt, B. V. (2023). Hydrophilic polymers: Current trends and visions for the future. *Progress in Polymer Science*, *147*, 101753.
25. Aungst, B. J. (2000). Intestinal permeation enhancers. *Journal of pharmaceutical sciences*, *89*(4), 429-442.
26. Dugo, G., & Di Giacomo, A. (2002). *Citrus: the genus citrus*. CRC Press.
27. Rowe, R. C., Sheskey, P., & Quinn, M. (2009). *Handbook of pharmaceutical excipients*. Libros Digitales-Pharmaceutical Press.
28. Sharma, P., & Tailang, M. (2022). Primaquine-loaded transdermal patch for treating malaria: design, development, and characterization. *Future Journal of Pharmaceutical Sciences*, *8*(1), 43.
29. Shabbir, M., Sajid, A., Hamid, I., Sharif, A., Akhtar, M. F., Raza, M., Ahmed, S., Peerzada, S., & Amin, M. U. (2019). Influence of different formulation variables on the performance of transdermal drug delivery system containing tizanidine hydrochloride: in vitro and ex vivo evaluations. *Brazilian Journal of Pharmaceutical Sciences*, *54*, e00130.
30. Patnaik, S., Purohit, D., Biswasroy, P., Diab, W. M., & Dubey, A. (2022). Recent

advances for commedonal acne treatment by employing lipid nanocarriers topically. *International journal of health sciences*, *6*(S8), 180-205.

31. Siepmann, J., & Peppas, N. (2012). Modeling of drug release from delivery systems based on hydroxypropyl methylcellulose (HPMC). *Advanced drug delivery reviews*, *64*, 163-174.
32. Aggarwal, S., Agarwal, S., & Jalhan, S. (2013). Essential oils as novel human skin penetration enhancer for transdermal drug delivery: a review. *Int J Pharm Bio Sci*, *4*(1), 857-868.
33. Chen, J., Jiang, Q.-D., Chai, Y.-P., Zhang, H., Peng, P., & Yang, X.-X. (2016). Natural Terpenes as Penetration Enhancers for Transdermal Drug Delivery. *Molecules*, *21*(12), 1709.
34. Raut, S. V., Nemade, L. S., Desai, M. T., Bonde, S. D., & Dongare, S. U. (2014). Chemical penetration enhancers: for transdermal drug delivery systems. *Int J Pharm Rev Res*, *4*, 33-40.
35. Mendonsa, N. S., Thipsay, P., Kim, D. W., Martin, S. T., & Repka, M. A. (2017). Bioadhesive drug delivery system for enhancing the permeability of a BCS class III drug via hot-melt extrusion technology. *AAPS PharmSciTech*, *18*(7), 2639-2647.
36. Nagra, U., Barkat, K., Ashraf, M. U., & Shabbir, M. (2022). Feasibility of enhancing skin permeability of acyclovir through sterile topical lyophilized wafer on self-dissolving microneedle-treated skin. *Dose-Response*, *20*(2), 15593258221097594.
37. Shabbir, M., Barkat, K., Ashraf, M. U., & Nagra, U. (2023). Development of a novel self-dissolving microneedle-assisted percutaneous delivery system of diacerein through solid dispersion gel: solubility enhancement, proof of anti-inflammatory activity and safety. *Current Drug Delivery*, *20*(9), 1351-1367.
38. Shabbir, M., Barkat, K., Ashraf, M. U., Nagra, U., & Shah, S. N. H. (2023). Assessment of formulation variables of poor water soluble diacerein for its improved loading and anti-inflammatory activity. *Drug Delivery and Translational Research*, *13*(6), 1780-1798.
39. Skotnicki, M., Aguilar, J. A., Pyda, M., & Hodgkinson, P. (2015). Bisoprolol and bisoprolol-valsartan compatibility studied by differential scanning calorimetry, nuclear magnetic resonance and X-ray powder diffractometry. *Pharmaceutical Research*, *32*(2), 414-429.
40. Kim, M.-H., Kim, D. H., Nguyen, D.-T., Lee, H. S., Kang, N.-W., Baek, M.-J., An, J., Yoo, S.-Y., Mun, Y.-H., & Lee, W. (2020). Preparation and evaluation of Eudragit L100-PEG proliponiosomes for enhanced oral delivery of celecoxib. *Pharmaceutics*, *12*(8), 718.
41. Kishore, R. S., Pappenberger, A., Dauphin, I. B., Ross, A., Buergi, B., Staempfli, A., & Mahler, H.-C. (2011). Degradation of polysorbates 20 and 80: studies on thermal autoxidation and hydrolysis. *Journal of pharmaceutical sciences*, *100*(2), 721-731.
42. Parikh, T., Gupta, S. S., Meena, A., & Serajuddin, A. T. (2016). Investigation of thermal and viscoelastic properties of polymers relevant to hot melt extrusion-III: Polymethacrylates and polymethacrylic acid based polymers. *International Journal of Pharmaceutical Excipients*, *5*(1).